

See discussions, stats, and author profiles for this publication at: <https://www.researchgate.net/publication/231633637>

# Steric Effects on the Adsorption of Alkylthiolate Self-Assembled Monolayers on Au (111)†

ARTICLE *in* THE JOURNAL OF PHYSICAL CHEMISTRY B · MARCH 2003

Impact Factor: 3.3 · DOI: 10.1021/jp021989+

---

CITATIONS

53

---

READS

24

4 AUTHORS, INCLUDING:



Qingfeng Ge

Southern Illinois University Carbondale

129 PUBLICATIONS 2,734 CITATIONS

SEE PROFILE

Steric Effects on the Adsorption of Alkylthiolate Self-Assembled Monolayers on Au (111)<sup>†</sup>Yanping Cao,<sup>‡</sup> Qingfeng Ge,<sup>§</sup> Daniel J. Dyer,<sup>‡</sup> and Lichang Wang<sup>\*‡</sup>*Department of Chemistry and Biochemistry, Southern Illinois University, Carbondale, Illinois 62901-4409, and Department of Chemical Engineering, University of Virginia, Charlottesville, Virginia 22904**Received: September 6, 2002; In Final Form: November 18, 2002*

Steric effects on the adsorption of self-assembled monolayers (SAMs) formed by alkylthiolates on the Au-(111) surface were investigated using density functional theory. Based on the ( $\sqrt{3} \times \sqrt{3}$ ) R30° structure, the current results on methylthiolate (CH<sub>3</sub>S) show that the adsorption prefers the face-centered cubic-bridge and hexagonal close-packed-bridge sites. Furthermore, the adsorption energy decreases slightly compared to the CH<sub>3</sub>S adsorption on the p(2 × 2) structure due to lateral interactions. Comparison between the results on CH<sub>3</sub>S and 1-propylthiolate (C<sub>3</sub>H<sub>7</sub>S) illustrates that the adsorption energy increases with chain length. Strong steric effects were found due to the chain length of the alkylthiolates and the hydrogen atoms in the CH<sub>2</sub> unit adjacent to the S atom ( $\alpha$  hydrogens). The energetically favored tilt angle is 20° for C<sub>3</sub>H<sub>7</sub>S. The preferred geometry for both CH<sub>3</sub>S and C<sub>3</sub>H<sub>7</sub>S adsorptions has the two  $\alpha$  hydrogens pointing toward the bridge Au atoms of the surface. The results suggest a flat potential energy surface, which correlates well with the dynamic nature of alkylthiolate SAMs observed experimentally.

## 1. Introduction

Self-assembled monolayers (SAMs) formed by the spontaneous assembly of alkylthiolates from solution onto gold provide a high degree of control over the chemistry and structure of an organic surface.<sup>1,2</sup> SAMs have been utilized in various technical applications, such as protective coatings,<sup>3</sup> friction and lubrication control,<sup>4</sup> adhesion,<sup>5</sup> building blocks in heterostructures and chemical anchors,<sup>6</sup> model systems for surface chemistry,<sup>7</sup> bio-related applications,<sup>8</sup> lateral structuring,<sup>9</sup> nonlinear optical applications,<sup>10</sup> and electronic applications.<sup>11</sup> The understanding of the adsorption kinetics, the structure of the binding site, and the geometry of the adsorbates are of fundamental interest to this field.

It is well-known that SAMs composed of alkylthiolates exhibit dynamic characteristics and may exhibit multidomain structures on gold. Is this solely due to the conformational mobility of the alkyl segments or does the distribution of binding sites also play a role? For instance, multiple binding sites could yield multidomained substrates, whereas a low energy global minimum would be expected to yield a single binding site that would favor a single domain. Theoretical studies can provide insights to help explain the morphology and structural dynamics of SAMs.

Established computational techniques, such as electronic structure, molecular dynamics, and Monte Carlo simulations, have been used to study SAMs.<sup>9</sup> Molecular dynamics and Monte Carlo simulations had been the principal computational tools in this area because of the complexity of SAMs, although the lack of accurate potential energy surfaces used in these calculations greatly affects the accuracy of the results. On the other hand, a number of electronic structure calculations were

performed to study sulfur–gold bond length, sulfur–sulfur spacing, adsorption site preference, and the tilt angle of the adsorbed molecules.<sup>12–21</sup> Among various electronic structure calculations, density functional theory (DFT) calculations have become the most popular tool in the studies of SAMs.<sup>15–21</sup> In studies of the adsorption of methylthiolate with very dilute coverage, Grönbeck et al. found a very strong sulfur–gold bond, a preference for the face-centered cubic (fcc) adsorption site, and alignment of the S–C bond along the surface normal.<sup>17</sup> The DFT calculations by Yourdshahyan et al.<sup>18</sup> also show the preferred adsorption is the fcc site at a range of coverages. Hayashi et al. studied methylthiolate adsorption at both dilute and dense coverages.<sup>19</sup> They found that methylthiolate binds in a strongly tilted configuration at the bridge (brd) site of the Au(111) surface with a reduced sulfur–gold bond strength compared to that of Grönbeck et al. They also demonstrated that numerical issues are responsible for this discrepancy in the energetics. In contrast, Gottschalck et al. reported the fcc-brd site as the preferred adsorption site for methylthiolate.<sup>21</sup>

Among these DFT studies, only the simplest alkylthiolate, i.e., methylthiolate (CH<sub>3</sub>S–), was investigated, but the alkylthiolate SAMs synthesized experimentally often consist of more than sixteen carbon atoms. To interpret our experimental observations, one needs to investigate adsorptions of alkylthiolates of longer chain lengths than methylthiolate. In addition, most of these DFT calculations are based on the p(2 × 2) structure corresponding to a coverage of 1/4. However, the c(4 × 2) superlattice of a ( $\sqrt{3} \times \sqrt{3}$ ) R30° hexagonal lattice is found in experiments.<sup>22–24</sup> Though it may not affect the preferred adsorption site, the p(2 × 2) structure may yield a different tilt angle than the ( $\sqrt{3} \times \sqrt{3}$ ) R30° structure due to strong lateral chain–chain interactions. Our primary objectives in this work are to investigate the preferred adsorption site, tilt angle, and other effects on the adsorption of alkylthiolates on the ( $\sqrt{3} \times \sqrt{3}$ ) R30° structure using 1-propylthiolate (C<sub>3</sub>H<sub>7</sub>S) as a probing molecule. Although 1-propylthiolate is shorter than the alkylthiolates used in experiments, the two CH<sub>2</sub> units would

<sup>†</sup> This paper is dedicated to James W. Neckers on the occasion of his 100<sup>th</sup> birthday.

<sup>\*</sup> To whom correspondence should be addressed. E-mail: lwang@chem.siu.edu. Phone: 618-453-6476. Fax: 618-453-6408.

<sup>‡</sup> Southern Illinois University.

<sup>§</sup> University of Virginia.

**TABLE 1: Adsorption Energies (eV/Molecule) of CH<sub>3</sub>S Monolayers on the Au(111) Surface with Different Slab Layers and *k* Points at Six Fixed Vacuum Layers**

slab layers	<i>k</i> points			
	1 × 1	3 × 3	5 × 5	7 × 7
1	−1.43	−0.51	−0.65	−0.60
2	−0.11	−1.20	−1.34	−1.29
3	−0.05	−1.27	−1.31	−1.32
4	−0.03	−1.30	−1.30	−1.38
6	0.077	−1.34	−1.38	−1.36

allow us to study major characteristics that are present in alkylthiolates of longer chains and to further elucidate experimental observations on these SAMs.

## 2. Method

Our calculations were carried out within the framework of DFT with a plane-wave basis set, encoded in the Vienna Ab Initio Simulation Package (VASP).<sup>25</sup> Ultrasoft pseudopotentials<sup>26</sup> are used to describe the electron–ion interaction. The wave functions are expanded in a plane-wave basis set with a cutoff energy of 320 eV,<sup>27</sup> and the Perdew–Wang 91 form of the generalized gradient approximation (GGA)<sup>28</sup> is used for describing the exchange and correction energies. Iterative matrix-diagonalization schemes with an efficient Pulay/Broyden-mixing scheme for the charge density are used to solve the Kohn–Sham equation self-consistently.

The gold surface was represented using a three layer slab, which is based on our testing results shown in Table 1. The Brillouin zone of the surface unit cell is sampled by a *k*-points grid of 5 × 5 (see Table 1). We used 6 vacuum layers in our simulations which are shown to be sufficient from our tests. The calculated energy differences between binding energies at different sites are converged to within 50 meV (about 1kcal/mol) although the absolute value of the calculated binding energy of a specific site may not be as accurate, as shown in Table 1.

In all simulations, Au atoms in the unit cell are fixed, which is demonstrated to have no significant effects on the results.<sup>21</sup> Furthermore, methylthiolate and 1-propylthiolate molecules are adsorbed on one side of the slab in a ( $\sqrt{3} \times \sqrt{3}$ ) R30° unit cell surface that corresponds to a coverage of 1/3, and these adsorbed molecules are fully relaxed. Although the c(4 × 2) superstructure has been observed experimentally,<sup>22,23,24</sup> it has been shown that the difference between the binding energies of CH<sub>3</sub>S in a ( $\sqrt{3} \times \sqrt{3}$ ) R30° structure and a c(4 × 2) superlattice is extremely small.<sup>20</sup> We note that chain length may have some effect on the ordering of the structure, as many more degrees of freedom are introduced in a long chain adsorption system. A systematic study on the effects of chain length and end-group is in progress.

The adsorption or the binding energy ( $E_b$ ), the energy required for removing the adsorbed molecule from the surface, is calculated by

$$E_b = E_t - E_c - E_m \quad (1)$$

where  $E_t$ ,  $E_c$ , and  $E_m$  are the total energy of the adsorption system, the metal slab, and the isolated molecule, respectively.

## 3. Results and Discussion

We begin by presenting our results on the preferred adsorption sites in the ( $\sqrt{3} \times \sqrt{3}$ ) R30° structure, as a good understanding of the adsorption site is critical for predicting the overall geometry and packing of the adsorbed organic thiolates; this

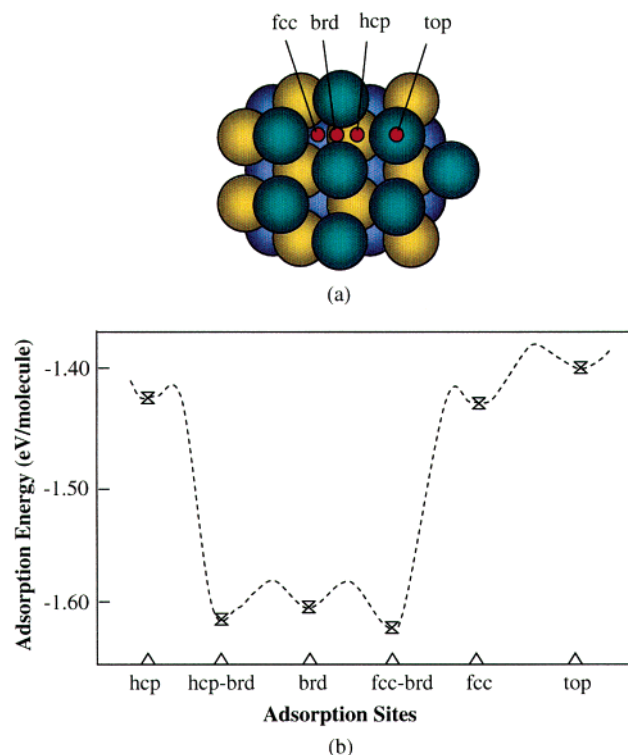


**Figure 1.** (a) Schematic representation of adsorption sites on Au (111). We use fcc, brd, and hcp to represent the face-centered cubic site, bridge site, and hexagonal close-packed site, respectively. (b) Adsorption energies versus adsorption sites for methylthiolate. The dashed curve is to assist connections among various adsorption sites.

will also play a critical role in the development of functional organic surfaces. Methylthiolate is used in this simulation for studies of the adsorption site. Our results show that methylthiolate prefers to occupy sites in the vicinity of the bridge site, and the adsorbed molecules experience a rather flat potential energy surface. Additional CH<sub>2</sub> groups should not alter the preferred binding site, as the change in energy would be similar for all binding sites. In the following section, we will present the results of the adsorption of 1-propylthiolate on Au (111) focusing on steric effects.

**3.1. Adsorption Site.** We have calculated adsorption energies at six different sites for the CH<sub>3</sub>S/Au system. They are the top, hexagonal close-packed (hcp), fcc, brd, and two bridge-like sites that are shown in Figure 1a. The adsorption geometries and energies of methylthiolate on these sites are given in Table 2. We note that the adsorption configurations shown in Table 2 are not the most stable ones for a given adsorption site. In Figure 1b, we plot the adsorption energies at different sites with the most stable configuration. Apparently, the most stable binding site lies in the vicinity of the bridge site with both the fcc–brd and hcp–brd sites being almost equally stable. There is a barrier of only about 0.03 eV between the fcc–brd and hcp–brd sites if the adsorbed methylthiolates diffuse through the bridge site from one to the other. Furthermore, the difference in binding energy between the fcc–brd and hcp–brd sites is so small that these two sites are essentially degenerate. We expect that this degeneracy is one of the reasons for multidomain formation in self-assembled monolayers as observed experimentally.<sup>29</sup> The initial adsorption of alkylthiolates on a clean Au(111) surface may take place at either fcc–brd or hcp–brd sites with almost equal probability. However, the growth of the monolayer structure in the vicinity of these initially adsorbed alkylthiolates will be limited by the available sites. This means that the incoming alkylthiolates will occupy the neighboring fcc–brd

**TABLE 2: Adsorption Energies and Geometries of CH<sub>3</sub>S Monolayers at Different Adsorption Sites on the Au(111) Surface**

Adsorption site <sup>1</sup>	Adsorption energy (eV/molecule)	Tilt angle (degrees)	C-S(Å)	S-Au(Å)
Top	-0.45	0	1.831	2.448
Fcc	-1.31	0	1.841	2.543(3) <sup>2</sup>
Fcc-brd	-1.39	10.8	1.851	2.565(2);2.622
Brd	-1.12	0	1.836	2.492(2)
Hcp-brd	-1.36	10.6	1.848	2.563(2);2.634
Hcp	-1.29	0	1.844	2.571(3)

<sup>1</sup> The CH<sub>3</sub>S is initially placed at a zero tilt angle and the system is subjected to a symmetry constraint. <sup>2</sup> The number in the parentheses represents the number of bonds of the same length.

sites when they are adsorbed close to an fcc-brd adsorbate. On the other hand, the incoming alkylthiolates will occupy the hcp-brd sites when they are adjacent to hcp-brd adsorbates. Therefore, different domains will form based on the initial binding sites. Furthermore, the distribution of domains will depend on the distribution of initial binding sites.

The C-S bond of the adsorbed CH<sub>3</sub>S is also stretched as shown in Table 2. Furthermore, the results demonstrate that the C-S bond distance increases with the strength of adsorption. Nevertheless, the distance from the sulfur atom to the Au atoms is correlated more to the local geometry of the adsorption site but less to the adsorption strength.

The current results on the preferred adsorption site on the ( $\sqrt{3} \times \sqrt{3}$ ) R30° unit cell agree with those obtained on a p(2 × 2) unit cell from our current calculation and by Gottschalck et al.<sup>21</sup> This indicates that the preferred sites are indeed not altered upon increasing the coverage of the methylthiolate species. Although the preferred adsorption site is not affected by the surface coverage, we do observe changes in adsorption energies upon increases in coverage. In the p(2 × 2) structure, the adsorption energy is 1.74 eV/molecule, which is in agreement with the previous result.<sup>21</sup> This value decreases to 1.62 eV/molecule obtained for a ( $\sqrt{3} \times \sqrt{3}$ ) R30° structure. This decrease, due to the increase in surface coverage, could be easily understood by the increased repulsion in the lateral interactions. Our results are in general agreement with that of Hayashi et al.<sup>19</sup> and Vargas et al.<sup>20</sup> These authors showed that the adsorption energies increase inversely with the coverage, and the site preference remains unchanged with coverage. However, the two most stable adsorption sites, hcp-brd and fcc-brd, were not investigated in those studies.<sup>19,20</sup>

Finally, it should be noted that the results obtained in this work are based on a perfect Au (111) surface. Very recent results by Molina and Hammer show that surface defects could play important roles in the adsorption structures and resulting domains.<sup>30</sup>

**3.2. Steric Effects.** There are three steric effects that greatly affect adsorption of alkylthiolate SAMs. The first steric effect is the tilt angle ( $\alpha$ ), as depicted in Figure 2. Measurements of tilt angles of SAMs have been the major focus of many experimental and theoretical studies, as it is a crucial factor in the development of functional SAMs. Most experimental results demonstrated that the tilt angles range from 20 to 35° by a variety of techniques, including ellipsometry, electron diffrac-

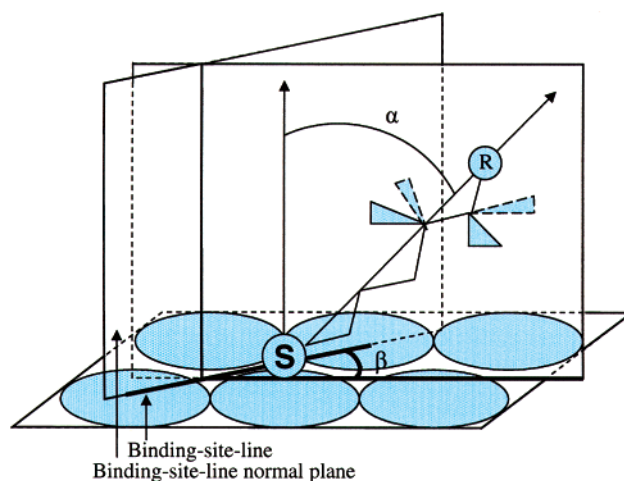


**Figure 2.** Schematic representation of an organic thiolate on the Au (111) surface.  $\alpha$  is the tilt angle of the molecule from the surface normal;  $\beta$  is the azimuthal angle between the molecular surface normal and the binding site-line surface normal planes; R=H, CH<sub>2</sub>, CH<sub>3</sub>, etc.

tion, IR, and Raman spectroscopy.<sup>31,32</sup> The molecular dynamics calculations based on the hcp site of the Au(111) ( $\sqrt{3} \times \sqrt{3}$ ) R30° structure reported tilt angles ranging from 30 to 35°. <sup>9,33</sup> More accurate DFT calculations on the tilt angle, however, studied the adsorption of methylthiolate on a p(2 × 2) unit cell with a coverage of 1/4; this coverage will greatly affect the tilt angle compared to the ( $\sqrt{3} \times \sqrt{3}$ ) R30° unit cell.<sup>18,21</sup> To better mimic experimental conditions, we chose 1-propylthiolate as the adsorbate to study the tilt angle on the ( $\sqrt{3} \times \sqrt{3}$ ) R30° Au(111) substrate.

The second steric effect is reflected by the azimuthal angle  $\beta$  as illustrated in Figure 2. The adsorption will vary depending on the azimuthal angle, as the relative geometric arrangement or distances between adsorbate atoms and Au atoms change at different azimuthal angles. The third steric effect appears when alkylthiolates consist of more than two carbon atoms. Although the molecular plane shown in Figure 2 is perpendicular to the Au surface, it can, in principle, tilt away from the surface normal plane. We define this angle as the molecular plane tilt angle,  $\gamma$ . Studies become more complicated if this effect is also taken into account. Therefore, all of the results reported here were obtained with the molecular plane perpendicular to the Au surface.

Rotation of the alkylthiolates around the surface will certainly affect adsorption processes because of the characteristics of the substrate. Figure 3a shows schematically two azimuthal angles; the left and right pictures show the molecular plane perpendicular and parallel to the binding-site-line, respectively. Furthermore, the azimuthal angle in the right picture of Figure 3a is 180°. Because of the symmetry of the Au surface studied here, the effect of azimuthal angles will be repeated at every 120°. In other words, the surface symmetry makes three complete cycles through a 360° rotation.

These steric effects are largely dependent on three parameters. The adsorption direction of the two hydrogen atoms of the CH<sub>2</sub> unit adjacent to the sulfur atom (defined here as  $\alpha$  hydrogens), the orientations of the remaining alkyl groups, which is more closely related to the chain length, and the adsorption site. In the case of CH<sub>3</sub>S, we can choose any two of the three hydrogen atoms as the  $\alpha$  hydrogens. We expect that the adsorption energies will be different depending on whether the  $\alpha$  hydrogens are closer to, or further away from the Au surface, as illustrated in Figure 3b.



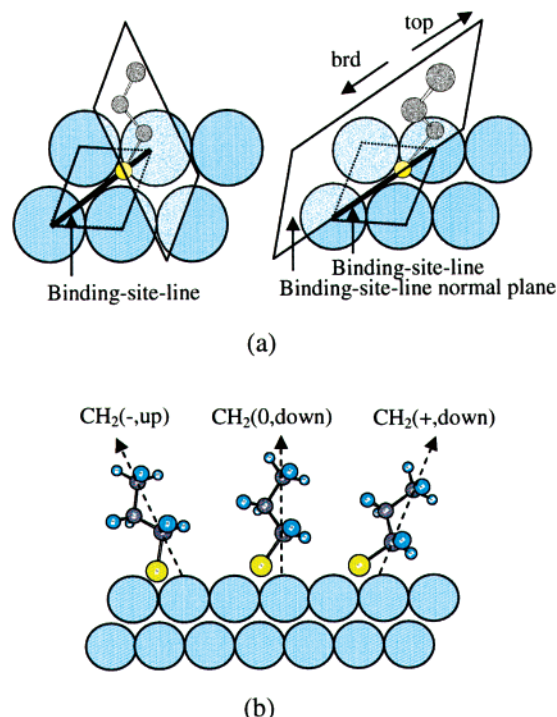


**Figure 3.** Schematic representations of 1-propylthiolate adsorption on the Au(111) surface. (a) The molecular plane is perpendicular (left) and parallel (right) to the binding site line normal plane. (b) Two opposite tilting directions with respect to the  $\alpha$  hydrogens, corresponding to positive tilt angles when the  $\alpha$  hydrogens point down and to negative tilt angles when the  $\alpha$  hydrogens point up.

**TABLE 3: Adsorption Energies of  $\text{CH}_3\text{S}$  at the fcc-brd Site of the Au (111) Surface at Different Tilt Angles**

system	tilt angle (degrees)	adsorption energy (eV/molecule)
1	-58	-1.36
2	0	-1.31
3	10.8	-1.39
4	46	-1.54
5	56	-1.62

To investigate the steric effects described above, we performed a series of studies on the adsorption of  $\text{CH}_3\text{S}$  and  $\text{C}_3\text{H}_7\text{S}$  on the  $(\sqrt{3} \times \sqrt{3})\text{R}30^\circ$  unit cell substrate. Before we discuss the results on the adsorption of  $\text{C}_3\text{H}_7\text{S}$ , we first present the results on the  $\text{CH}_3\text{S}$  adsorption. In particular, we concentrate here on the surface coverage effect on the tilt angle, which is measured between the C–S bond axis and the surface normal. The results in Table 3 show that the preferred tilt angle on the  $(\sqrt{3} \times \sqrt{3})\text{R}30^\circ$  structure is  $56^\circ$ , whereas that on the  $\text{p}(2 \times 2)$  structure is  $58^\circ$ , which is in good agreement with the previous study.<sup>21</sup> This small decrease indicates that the coverage increase from 1/4 to 1/3 does not exhibit a large impact on the tilt angle. This angle shown in Table 3 should not be confused with the tilt angle for longer chain alkylthiolates as defined in Figure 2. To make a consistent comparison, we also measured the angle between the C–S bond and the surface normal for the most stable  $\text{C}_3\text{H}_7\text{S}$  adsorption. This angle,  $53^\circ$ , is only slightly smaller than  $56^\circ$  of the adsorbed  $\text{CH}_3\text{S}$ . The small decrease in angle with increasing chain length may be attributed to the modification of the S–Au interactions, as a hydrogen atom is replaced with an alkyl group (R).

To further explore the steric effect, we investigated the  $\text{C}_3\text{H}_7\text{S}$  adsorption at two azimuthal angles, 0 and  $60^\circ$ , and various tilt angles. The results are also provided in Table 4. It is clear that the most stable tilt angle depends on the azimuthal angle. Figure

**TABLE 4: Adsorption Energies of  $\text{C}_3\text{H}_7\text{S}$  on the Au(111) Surface at Different Tilt Angles ( $\alpha$ ) and at Two Azimuthal Angles ( $\beta$ )<sup>a</sup>**

$\beta(^{\circ})$	$\alpha(^{\circ})$	adsorption energy (eV/molecule)	S–Au ( $\text{\AA}$ )
0	-50.3	-1.36	2.612,2.614,2.487
	-46.0	-1.37	2.525,2.527,2.550
	-41.2	-1.37	2.520,2.522,2.551
	-36.4	-1.38	2.518,2.520,2.557
	-31.5	-1.38	2.516,2.519,2.559
	-26.4	-1.39	2.515,2.517,2.564
	-17.3	-1.43	2.521,2.523,2.595
	-8.0	-1.48	2.524,2.526,2.641
	1.2	-1.54	2.524,2.528,2.704
	9.9	-1.60	2.527,2.529,2.815
	19.8	-1.64	2.531,2.532,2.894
	26.1	-1.62	2.545,2.545,3.051
	29.7	-1.59	2.546,2.546,3.148
	50	-1.37	2.515,2.512,2.646
	45.9	-1.38	2.537,2.535,2.530
	41.2	-1.39	2.540,2.538,2.517
	36.4	-1.39	2.540,2.539,2.510
	31.4	-1.39	2.543,2.541,2.506
	26.4	-1.40	2.545,2.543,2.503
	16.4	-1.43	2.519,2.519,2.519
60	-6.9	-1.46	2.563,2.562,2.528
	3.6	-1.48	2.570,2.568,2.586
	15.6	-1.48	2.608,2.607,2.742
	26.7	-1.41	2.632,2.630,2.804
	29.1	-1.40	2.878,2.878,2.485
	30.4	-1.37	2.688,2.687,2.716

<sup>a</sup> Initially, the  $\text{C}_3\text{H}_7\text{S}$  is placed at the fcc site and is fully relaxed.

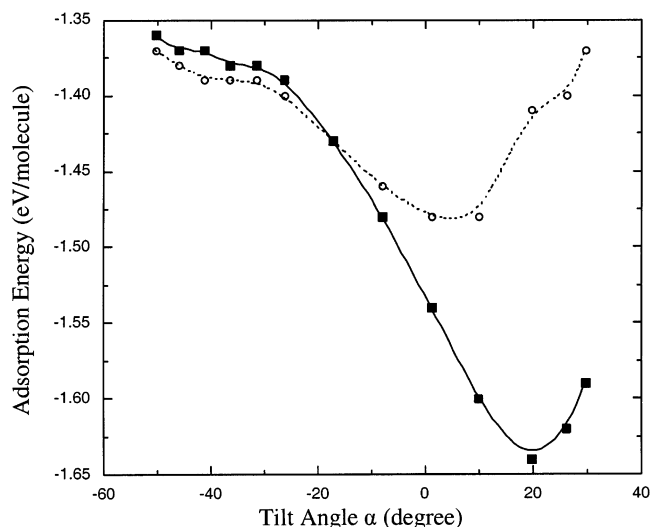


**Figure 4.** Adsorption energies versus tilt angles ( $\alpha$ ) for 1-propylthiolate plotted using the data from Table 4. The solid curve represents the  $\alpha$  hydrogens pointing in the brd direction ( $\beta = 0$ ), whereas the dash curve represents the  $\alpha$  hydrogens pointing in the top direction ( $\beta = 60^\circ$ ).

4 depicts the adsorption energies as a function of tilt angles at these azimuthal angles.

These results demonstrate that the preferred tilt angle is about  $20^\circ$  when the  $\alpha$  hydrogens point toward the bridge site ( $\beta = 0$ ). However the preferred tilt angle is about  $10^\circ$  when the  $\alpha$  hydrogens point toward the top site ( $\beta = 60^\circ$ ). Furthermore, at both fixed azimuthal angles, our results show that the most stable adsorption prefers the  $\alpha$  hydrogens pointing toward the Au surface.

Finally, it is worth mentioning the possibility that the molecular plane may also be tilted by an angle ( $\gamma$ ) with respect to the surface. Our results are obtained at  $\gamma = 0$ ; that is, the molecular plane is normal to the substrate. However, such a

tilt might have a profound effect on the homogeneity of the SAM surface and the adsorption of chiral molecules. For instance, a tilt of the molecular plane would create a chiral system with enantiomorphous domains (i.e., left and right tilted), even if the molecules were achiral. Thus, the interaction energy between a chiral molecule and the right or left tilted domains would be different, because their relationship is diastereomeric when  $\gamma \neq 0$ . A fundamental understanding of these interactions is an important goal in contemporary surface science. Work is in progress to elucidate steric as well as chiral effects.

#### 4. Conclusions

Simulations based on DFT were performed to model SAMs formed by alkylthiolates on the Au (111) substrate. First, the simulations suggest that the fcc-brd and hcp-brd sites are the preferred adsorption sites for the adsorption on a ( $\sqrt{3} \times \sqrt{3}$ ) R30° unit cell which corresponds to a coverage of 1/3. We found that the adsorption energy decreases slightly due to an increase in the surface coverage but increases with the chain length of the adsorbed alkylthiolates. Furthermore, many local minima exist because of the coupling of different degrees of freedom of the adsorption system. Second, the strongest adsorption for C<sub>3</sub>H<sub>7</sub>S occurs at zero azimuthal angle with the two  $\alpha$  hydrogens pointing toward the bridge Au atoms of the surface. In addition, the preferred tilt angle for the 1-propylthiolate is 20°. Our results also indicate that the tilt angle decreases slightly with an increase in surface coverage. However, the difference in adsorption energies is small among different adsorption configurations, which suggests a relatively flat potential energy surface. As a result, entropic contributions from the organization of the adlayer will have strong influences on the final ordering of SAMs; therefore, the formation of multiple domains is predicted.

**Acknowledgment.** D.J.D. thanks the National Science Foundation under Grant CHE-0094195 and the Materials Technology Center at SIUC for partial support of this work. L.W. thanks SIUC for startup funds and the National Partnership for Advanced Computational Infrastructure under Grant CHE020006 for providing partial computational times on the Blue Horizon.

#### References and Notes

- (1) Ulman, A. *Chem. Rev.* **1996**, *96*, 1533.
- (2) Bain, C. D.; Troughton, E. B.; Tao, Y.-T.; Evall, J.; Whitesides, G. M.; Nuzzo, R. G. *J. Am. Chem. Soc.* **1989**, *111*, 321.
- (3) Scherer, J.; Vogt, M. R.; Magnussen, O. M.; Behm, R. J. *Langmuir* **1997**, *13*, 7045.
- (4) Xiao, X.; Hu, J.; Charych, D. H.; Salmeron, M. *Langmuir* **1996**, *12*, 235.
- (5) Kim, S.; Choi, G. Y.; Ulman, A.; Fleischer, C. *Langmuir* **1997**, *13*, 6850.
- (6) Jordan, R.; Ulman, A. *J. Am. Chem. Soc.* **1998**, *120*, 243.
- (7) Finklea, H. O.; Bard, A. J.; Rubinstein, I. *Electroanalytical Chemistry*; Marcel Dekker: New York, 1996.
- (8) Prime, K. L.; Whitesides, G. M. *Science* **1991**, *252*, 1164.
- (9) Ulman, A. *Self-assembled monolayers of thiols, Thin Films*; Academic Press: San Diego, 1998; Vol. 24.
- (10) Ulman, A. *An Introduction to Ultrathin Organic Films: From Langmuir-Blodgett to Self-Assembly*; Academic Press: Boston, 1991.
- (11) Vuillaume, D.; Boulas, C.; Collet, J.; Allan, G.; Delerue, C. *Phys. Rev. B* **1998**, *58*, 16491.
- (12) Schreiber, F. *Prog. Surf. Sci.* **2000**, *65*, 151.
- (13) Sellers, H. *Surf. Sci.* **1993**, *294*, 99.
- (14) Beardmore, K. M.; Kress, J. D.; Grønbeck-Jensen, N.; Bishop, A. R. *Chem. Phys. Lett.* **1998**, *286*, 40.
- (15) Sellers, H.; Ulman, A.; Shnidman, Y.; Eilers, J. E. *J. Am. Chem. Soc.* **1993**, *115*, 9389.
- (16) Akinaga, Y.; Nakajima, T.; Hirao, K. *J. Chem. Phys.* **2001**, *114*, 8555.
- (17) Grønbeck, H.; Curioni, A.; Andreoni, W. *J. Am. Chem. Soc.* **2000**, *122*, 3839.
- (18) Yourdshahyan, Y.; Zhang, H. K.; Rappe, A. M. *Phys. Rev. B* **2001**, *63*, 81405(R).
- (19) Hayashi, T.; Morikawa, Y.; Nozoye, H. *J. Chem. Phys.* **2001**, *114*, 7615.
- (20) Vargas, M. C.; Giannozzi, P.; Selloni, A.; Scoles, G. *J. Phys. Chem. B* **2001**, *105*, 9509.
- (21) Gottschalck, J.; Hammer, B. *J. Chem. Phys.* **2002**, *116*, 784.
- (22) Camillone, N., III.; Chidsey, C. E. D.; Liu, G.-Y.; Scoles, G. *J. Chem. Phys.* **1993**, *98*, 3503.
- (23) Doboys, L. H.; Zegarski, B. R.; Nuzzo, R. G. *J. Chem. Phys.* **1993**, *98*, 678.
- (24) Fenter, P.; Schreiber, F.; Berman, L.; Scoles, G.; Eisenberger, P.; Bedzyk, M. J. *Surf. Sci.* **1998**, *412/413*, 213.
- (25) (a) Kresse, G.; Hafner, J. *Phys. Rev. B* **1993**, *47*, 558. (b) Kresse, G.; Furthmüller, J. *Phys. Rev. B* **1996**, *54*, 11169. (c) Kresse, G.; Furthmüller, J. *Comput. Mater. Sci.* **1996**, *6*, 15.
- (26) Vanderbilt, D. *Phys. Rev. B* **1990**, *41*, 7892.
- (27) Ge, Q.; Neurock, M.; Wright, H. A.; Srinivasan, N. *J. Phys. Chem.* **2002**, *106*, 2826.
- (28) Perdew, J.; Chevary, J. A.; Vosko, S. H.; Jackson, K. A.; Pederson, M. R.; Singh, D. J.; Fiolhais, C. *Phys. Rev. B* **1992**, *46*, 6671.
- (29) (a) Poirier, G. E.; Tarlov, M. J.; Rushneier, H. E. *Langmuir* **1994**, *10*, 3383. (b) Poirier, G. E.; Tarlov, M. J. *Langmuir* **1994**, *10*, 2853.
- (30) Molina, L. M.; Hammer, B. *Chem. Phys. Lett.* **2002**, *360*, 264.
- (31) Strong, L.; Whitesides, G. M. *Langmuir* **1988**, *4*, 546.
- (32) Bryant, M. A.; Pemberton, J. E. *J. Am. Chem. Soc.* **1991**, *113*, 8284.
- (33) Zhong, C. J.; Brush, R. C.; Anderegg, J.; Porter, M. D. *Langmuir* **1999**, *15*, 518.